Thangarajan Umamathi[1], Ramachandran Parimalam[1], Venkatachalam Prathipa[2], Antony Josephine Vanitha[1], Kalimuthu Muneeswari[1],Babu Mahalakshmi[1], Susai Rajendran[3,4], Anitha Nilavan[3]*

[1]Sri Meenakshi Government Arts College For Women (A), Department of Chemistry, Madurai , India,[2]PSNA College of Engineering and Technology, Department of Chemistry, Dindigul, Tamilnadu, India, [3]St. Antony's College of Arts and Sciences For Women, Corrosion Research Centre, Department of Chemistry, Dindigul,Tamilnadu, India, [4]Pondicherry University, Centre for Nanoscience and Technology, Puducherry, India

Scientific paper
ISSN 0351-9465, E-ISSN 2466-2585
https://doi.org/10.5937/zasmat2203341U

Zastita Materijala 63 (3)
341 - 352 (2022)

Influence of urea and glucose on corrosion resistance of Gold 21K alloy in the presence of artificial sweat

ABSTRACT

Corrosion resistance of Gold 21K alloy immersed in artificial sweat in the absence and presence of 100 ppm of urea and also 100 ppm of D-Glucose has been investigated by polarization study and AC impedance spectra. It is observed that Corrosion resistance of Gold 21K alloy immersed in artificial sweat in the presence of 100 ppm of urea / D-Glucose increases. Hence it is concluded that people wearing ornaments made of Gold 21K alloy need not worry about the excess of urea / D-Glucose in their sweat. When Gold 21K alloy is immersed in artificial sweat in the presence of 100 ppm of urea, Linear Polarisation Resistance value increases from 103389Ohmcm^2 to 123437Ohmcm^2; corrosion current decreases from 4.036 x10^{-7}A/cm^2 to 3.308 x10^{-7}A/cm^2; charge transfer resistance value increases from 10490 Ohmcm^2 to 14070 Ohmcm^2 ; impedance value increases from 4.253 to 4.324; double layer capacitance decreases from 4.862x10^{-10} F/cm^2 to 3.625x10^{-10} F/cm^2, and phase angle increases from 38.91 to 70.14. When Gold 21K alloy is immersed in artificial sweat in the presence of 100 ppm of D-Glucose, Linear Polarisation Resistance value increases from 103389Ohmcm^2 to 4817257Ohmcm^2; corrosion current decreases from 4.036 x10^{-7}A/cm^2 to 0.161x10^{-7}A/cm^2 ; charge transfer resistance increases from 10490Ohmcm^2 to 33300Ohmcm^2; impedance value increases from 4.253 to 4.977; double layer capacitance decreases from 4.862x10^{-10} F/cm^2 to 1.5315x10^{-10} F/cm^2, and phase angle increases from 38.91° to 79.74°.

Keywords: *Corrosion resistance, Thermo active alloy, Gold 21K alloy, Artificial sweat, polarization study, AC impedance spectra.*

1. INTRODUCTION

Metals and alloys after implantation, come in contact with several body fluids. After implantation they undergo corrosion in the environments of the body fluids. Corrosion resistance of several alloys in many body fluids has been studied by several researchers [1-10].

Wang et al. [1] have studied Tribo-corrosion mechanisms and electromechanical behaviors for metal implants materials of CoCrMo, Ti6Al4V and Ti15Mo alloys. It has been reported that the Ti15Mo alloy would be the better alternative for metal implant applications compared with the CoCrMo alloy for the consideration of both wear and potential poisonous ions such as Co (III) and Cr(VI). In order to meet the clinical demand for titanium implants, the heterogeneous structure of TiO_2/$SrTiO_3$ coating was in situ fabricated on the surface of Ti_6Al_4V alloy by a facile way by Si et al. [2]. It is observed that a multifunctional coating system was proposed to provide inspiration for the development of novel artificial bone implant materials. Nanoflex stainless steel is a gifted material for medical applications. Nevertheless, improvement of its mechanical properties without compromising its corrosion resistance is still a challenge. In order to investigate the effect of the nitriding process on the corrosion and wear resistance of Sandvik Nanoflex™ steel, many processes were carried out in a gas atmosphere with differing ammonia contents in the temperature range of 425–475◦C for 4 h by Kochmański et al. [3]. It is concluded that nitriding should be carried out at a temperature below 450◦C and in an atmosphere containing no more than approximately

*Corresponding author:Thangarajan Umamathi
E-mail: umamathilesslie10@ gmail.com
Paper received: 30. 03. 2022.
Paper accepted: 14. 04. 2022.
Paper is available on the website: www.idk.org.rs/journal

50% ammonia in order to avoid nitrides precipitation.

Ti6Al4V is a widely used metal for biomedical application due to its excellent corrosion resistance, biocompatibility and mechanical strength. Nonetheless, a coupling reaction of friction and corrosion is the critical reason for the failure of implants during the long-term service in human body, shortening the life expectancy and clinical efficacy of prosthesis. So Lu et al [4] designed a study to find a feasible approach to modify the service performances of Ti6Al4V. It was found out that the combination of laser rescanning and Grapheme Oxide mixing can synergistically enhance the tribocorrosion properties of titanium alloy, which is a feasible way to prolong the service lives of medical implants. Corrosion behavior of Cu-Zn-Ni-Sn imitation-gold copper alloy in artificial seawater and perspiration has been investigated by Yu et al.[5]. Electrochemical behavior of various implantation biomaterials in the presence of various simulated body fluids has been investigated by Mary et al [6]. Elzohry et al.[7] have investigated chemical, electrochemical and corrosive wear behavior of nickel-plated steel and brass-plated steel based coins from Egypt. The corrosion behavior many of metallic materials used as jewelry in synthetic sweat solution was studied by electrochemical polarization method by Nasser et al [8]. Results showed that the sample (Cu-Fe alloy) has the majority corrosion potential in negative beside the highest current density as well as the current density reached to 366.13 $\mu A.cm^{-2}$, while Red brass has the noblest corrosion potential in addition the current density of corrosion is very low, and reached to 11.080 $\mu A.cm^{-2}$. The surface morphology of the surface of corroded specimens was analyzed using scanning electron microscope to show the product of corrosion with damage on the surface of the material. Atmospheric corrosion behavior of benzotriazole treated cu-based coins in synthetic sweat has been investigated by et al.[9]. Bio accessibility of nickel and cobalt in powders and massive forms of stainless steel, nickel- or cobalt-based alloys, and nickel and cobalt metals in artificial sweat has been investigated by Wang et al. [10].

Human perspiration (sweat) comes in contact with a number of consumer products. Contact can cause a variety of undesirable effects. Dyes can bleed or discolor, components can corrode and/or malfunction, residues can be unsightly. The problem of metal corrosion resulting from contamination by palmar sweat is common to many industrial occupations. Constant handling of metal parts by some individuals causes an accumulation of rust. In the manufacture of highly finished metal products, for example ball-bearings, and also in subsequent assembling and packing processes, serious consideration must be given to this effect. The corrosive nature of sweat has been known as early as 1919. But few objective investigations on this subject have appeared. Many ornaments such as wrist watches, chains, rings, and bangles etc., made of Gold 21K alloy may come in contact with sweat. The sweat of some people may contain excess of sodium chloride and urea. These chemicals, in addition to sweat, may cause the corrosion of Gold 21K alloy .The present work is undertaken to investigate the influence of sodium chloride and urea on the corrosion resistance of Gold 21K alloy in artificial sweat by electrochemical studies such as polarization study and AC impedance spectra.

2. EXPERIMENTAL

Preparation of the metal specimens

A thin wire of Gold 21K alloy is used as test material for this work. 21K gold consists of 21 parts of pure gold and 3 parts of other metals, or 87.5% of pure gold and 12.5% of other alloys. This level of gold purity is popular for plain jewellery mainly. Although it is a little more durable than 22K gold, its hardness is still not enough for heavy gemstones The Gold 21K alloy was encapsulated in Teflon rod. It was polished to mirror finish and used for electrochemical studies. The metal specimens encapsulated in a Teflon rod were immersed in artificial sweat (the ISO standard ISO 3160-2), whose composition was: 20g/l NaCl, 17.5 g/l NH_4Cl, 5g/l acetic acid and 15 g/l d,l lactic acid with the pH adjusted to 4.7 by NaOH.

Electrochemical study

In the present work corrosion resistance of Gold 21K alloy immersed in various test solutions were measured by Polarization study and AC impedance spectra (also known as EIS = Electro-chemical Impedance Spectra). In the present exploration, polarization studies were carried out in a CHI Electrochemical work station/ analyzer, model 660A.

Polarization study

Polarization studies were carried out in a three electrode cell assembly. A SCE was the reference electrode. Platinum was the counter electrode. Mild steel was the working electrode. From polarization study, corrosion parameters such as corrosion potential (E_{corr}), corrosion current (I_{corr}), Tafel slopes anodic = b_a, and cathodic = b_c ,and LPR (linear polarisation resistance) values were measured.

AC impedance spectra

In the present investigation the same instrument and set-up used for polarization study was used to record AC impedance spectra also. A time interval of 5 to 10 min was given for the system to attain a steady state open circuit potential. The real part (Z') and imaginary part (Z'') of the cell impedance were measured in ohms at various frequencies. AC impedance spectra were recorded with initial E(v)=0, high frequency (Hz = $1x10^5$), low frequency (Hz=1),amplitude (V)=0.005 and quiet time (s)=2. From Nyquist plot the values of charge transfer resistance (R_t) and the double layer capacitance (C_{dl}) were calculated. From Bode plots impedance values and phase angle values were calculated.

$$R_t=(R_s+R_t)- R_s$$

where R_s is solution resistance.

C_{dl} values were calculated using the relationship

$$C_{dl} = 1/ 2\times 3.14 \times R_t\times f_{max}$$

where f_{max} = frequency at maximum imaginary impedance.

3. RESULTS AND DISCUSSION

The present investigation is undertaken to study the corrosion resistance of ornaments such as wrist watch and ring made of Gold 21K alloy in artificial sweat in the absence and presence of urea (100 ppm) and also D-Glucose (100 ppm), by electrochemical studies such as polarisation study and AC impedance spectra [11-20].

Polarisation study

The influence of urea (100 ppm) and also D-Glucose (100 ppm), on the corrosion resistance of Gold 21 K alloy in artificial sweat (AS), has been investigated by polarization study.

The Polarization curves of Gold 21K alloy in AS in the absence and presence of of urea (100ppm) and also D-Glucose (100ppm) are shown in Figures 1-3. The corrosion parameters are given in Table1. The corrosion parameters are compared in Figures 4-6.

Table 1. Corrosion parameters of Gold 21K alloy immersed in various tests solutions obtained by polarization study

Tabela 1. Parametri korozije legure zlata 21K potopljene u različita ispitivanja rastvora dobijenih proučavanjem polarizacije

System	E_{corr} mV vs SCE	b_c mV/decade	b_a mV/decade	LPR Ohm cm^2	I_{corr} A/cm^2
Artificial sweat	25	199	186	103389 (3)	$4.036 x10^{-7}$
AS+ Urea , 00 ppm	110	192	184	123437(2)	$3.308 x10^{-7}$
AS+ Glucose, 100 ppm	-129	151	894	4817257(1)	$0.161x10^{-7}$

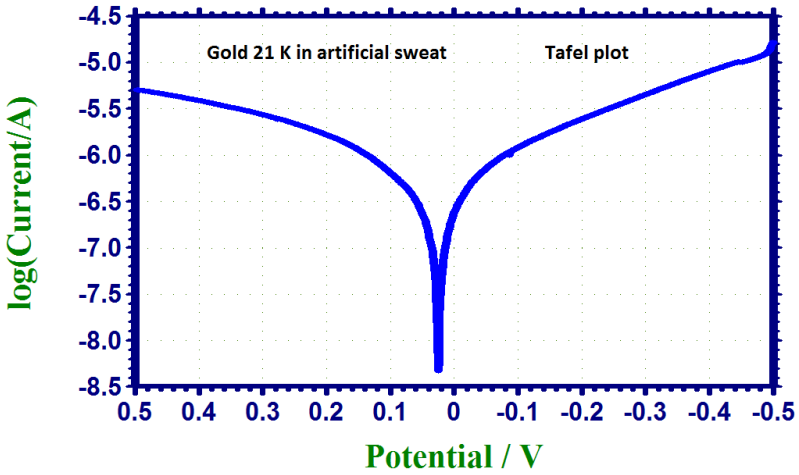

Figure 1. Polarization curve of Gold 21K immersed in artificial sweat (AS)

Slika 1. Kriva polarizacije zlata 21K uronjenog u veštački znoj (AS)

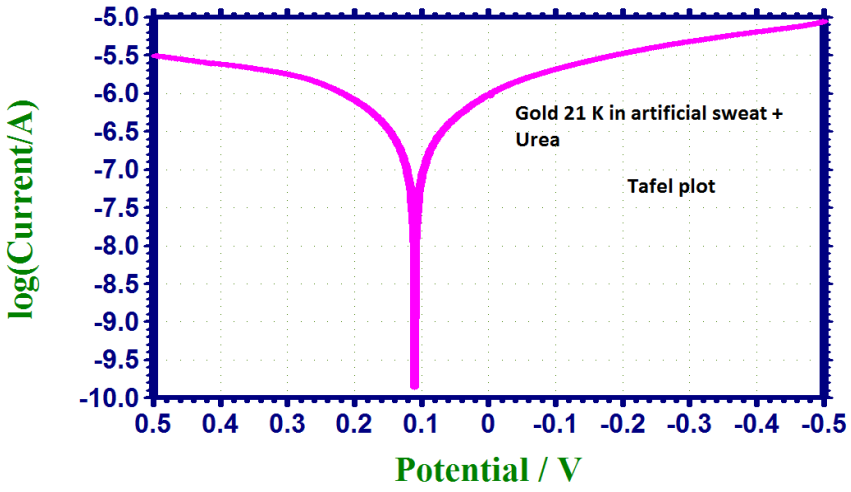

Figure 2. Polarisation curve of Gold 21K immersed in artificial sweat (AS) + Urea

Slika 2. Kriva polarizacije zlata 21K uronjenog u veštački znoj (AS) + urea

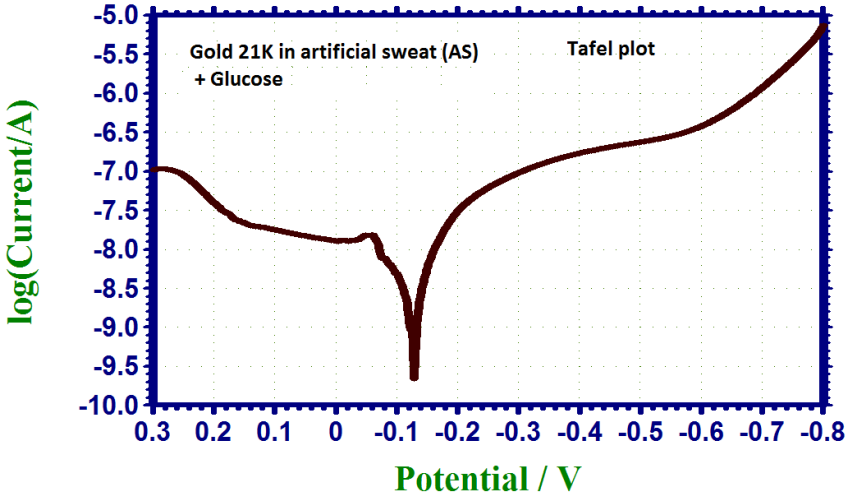

Figure 3. Polarisation curve of Gold 21K immersed in artificial sweat (AS) + Glucose

Slika 3. Kriva polarizacije zlata 21K uronjenog u veštački znoj (AS) + glukoza

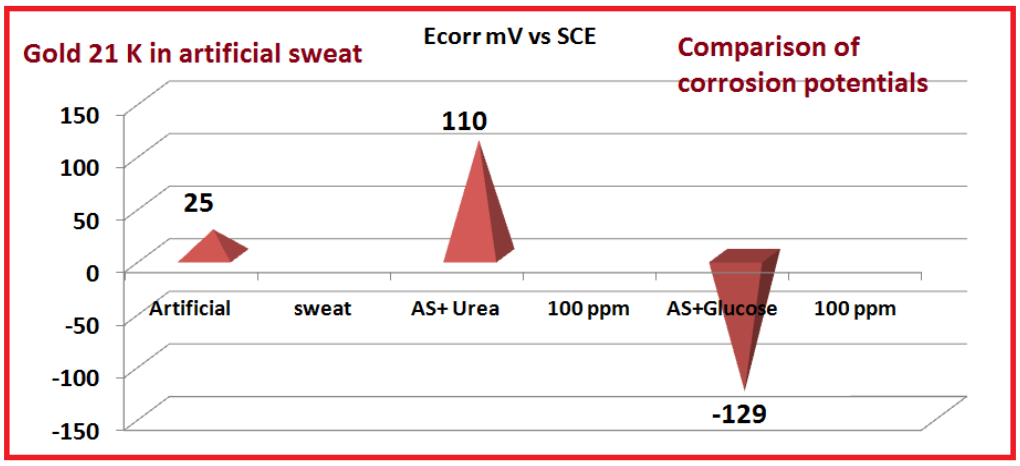

Figure 4. Comparison of corrosion potentials of Gold 21K immersed in various test solutions

Slika 4. Poređenje potencijala korozije zlata 21K uronjenog u različita testirana rešenja

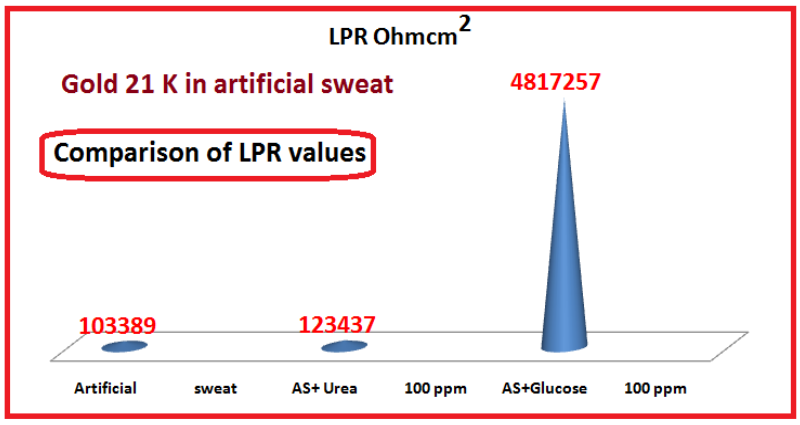

Figure 5. Comparison of LPR values of Gold 21K immersed in various test solutions

Slika 5. Poređenje LPR vrednosti zlata 21K uronjenog u različita testirana rešenja

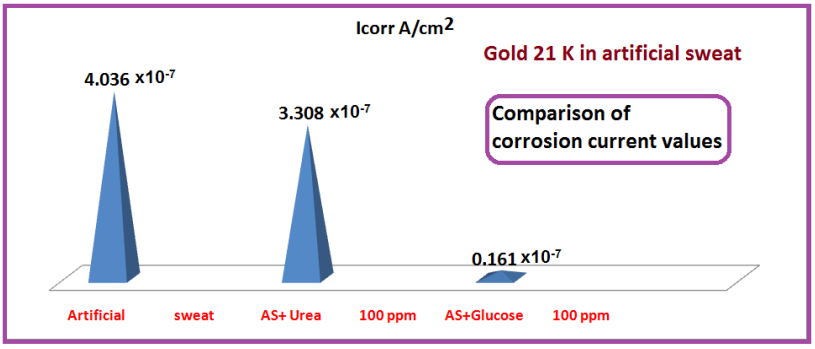

Figure 6. Comparison of corrosion current values of Gold 21K immersed in various test solutions

Slika 6. Poređenje vrednosti struje korozije zlata 21K uronjenog u različita testirana rešenja

In polarization study, when corrosion resistance increases, LPR increases and corrosion current decreases (Scheme A).

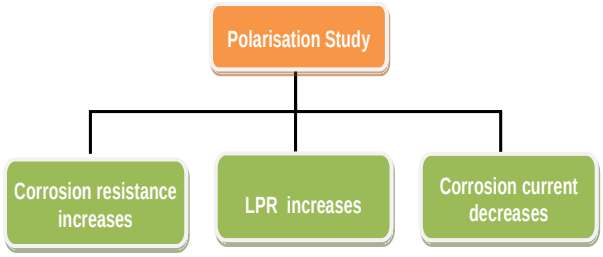

Scheme A. Correlation among corrosion parameters in polarization study

Šema A. Korelacija između parametara korozije u proučavanju polarizacije

Based on this concepts, it is observed from Table 1, that in the presence of 100 ppm of urea, the corrosion resistance of Gold 21K in AS increases. This is revealed by the fact that, in the presence of 100 ppm of urea, LPR value of Gold 21K increases (Figure 5) and corrosion current decreases (Figure 6).

It is also observed from Table 1, that in the presence of 100 ppm of Glucose, the corrosion resistance of Gold 21K in AS increases. This is revealed by the fact that, in the presence of 100ppm of Glucose, LPR value of Gold 21K increases (Figure 5) and corrosion current decreases (Figure 6).

It is also inferred that in the presence of urea the corrosion potential shifts from 25 to 110mV VS SCE (Figure 4). It is inferred that in presence of 100ppm of urea the anodic reaction is controlled predominantly.

It is also inferred that in the presence of Glucose, the corrosion potential shifts from 25 to -129mV VS SCE (Figure 4). It is inferred that in presence of 100 ppm of Glucose, the cathodic reaction is controlled predominantly.

Polarisation study leads to the conclusion that the corrosion resistance of Gold 21K in various test solution decreases in the following order:

Artificial sweat + Glucose > Artificial sweat + urea > Artificial sweat

Implication

Corrosion resistance of Gold 21K in artificial sweat increases in the presence of 100ppm of urea and also 100 ppm of glucose. Hence people having excess of urea/glucose in sweat need not worry about wearing ornaments made of Gold 21K alloy, such as wrist watches, rings, bangles etc.

AC Impedance spectra

The AC impedance spectra of Gold 21K alloy in AS in the absence and presence of 100ppm of urea and also 100ppm of glucose are shown in Figures 7-15.The Nyquist plots are shown in Figures 7,10 and 13. The Bode plots are shown in Figures 8, 9, 11, 12, 14 and 15. The corrosion parameters are compared in Figures 16 and 17.

The corrosion parameters such as change transfer resistance (Rt), impedance value and double layer capacitance (C_{dl}) values, impedance values and phase angle values are given in Table 2.

Table 2. Corrosion parameters of Gold 21K alloy immersed in various test obtained by AC impedance spectra

Tabela 2. Parametri korozije legure zlata 21K potopljene u različitim testovima dobijenim spektrom impedanse naizmenične struje

system	R_t Ohmcm^2	C_{dl} F/cm^2	Impedance Log (Z/ohm)	Phase Angle°
AS	10490	4.862x10-10	4.253	38.91
AS+ Urea 100 ppm	14070	$3.625x10^{-10}$	4.324	70.14
AS+ Glucose 100 ppm	33300	$1.5315x10^{-10}$	4.977	79.74

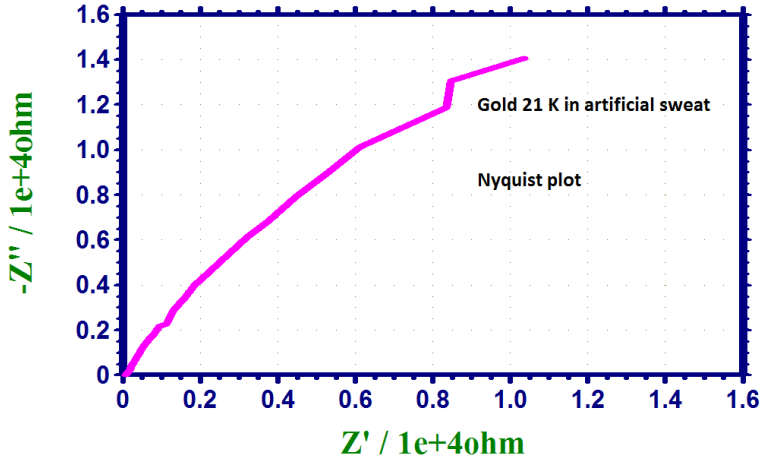

Figure 7. Nyquist plot of Gold 21K immersed in artificial sweat (AS)

Slika 7. Nyquist-ova kriva zlata 21K uronjena u veštački znoj (AS)

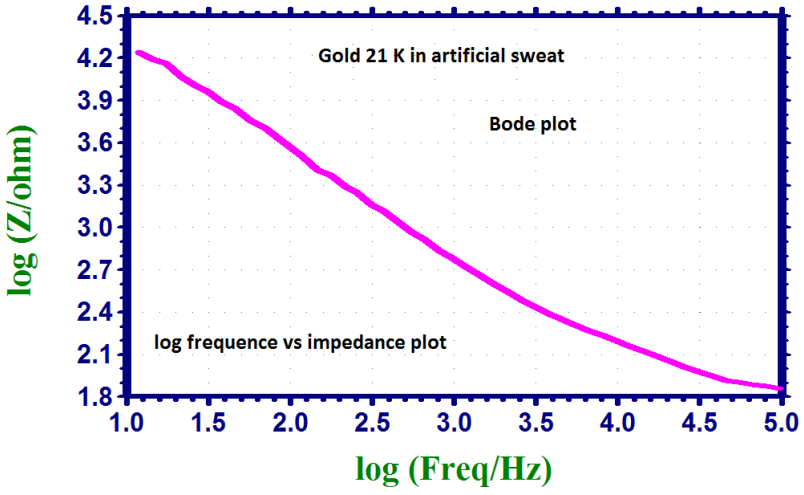

Figure 8. Log frequency vs. impedance plot of Gold 21K immersed in artificial sweat (AS)

Slika 8. Log frekvencije u odnosu na impedansu zlata 21K uronjenu u veštački znoj (AS)

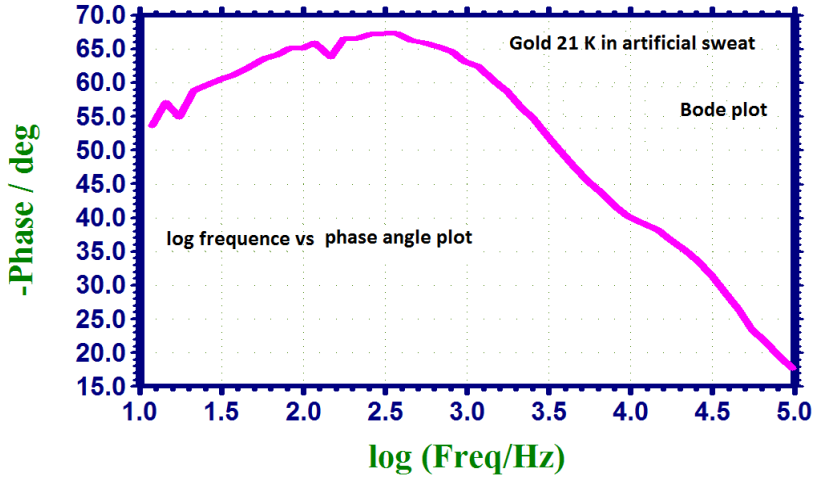

Figure 9. Log frequency vs. phase angle plot of Gold 21K immersed in artificial sweat (AS)

Slika 9. Log frekvencije u zavisnosti od faznog ugla zlata 21K uronjenog u veštački znoj (AS)

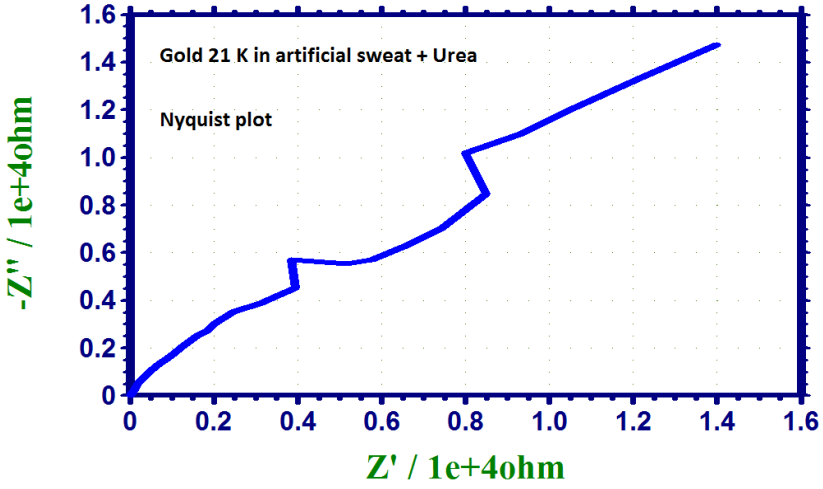

Figure10. Nyquist plot of Gold 21K immersed in artificial sweat (AS) + Urea

Slika 10. Nyquist-ova kriva zlata 21K uronjena u veštački znoj (AS) + urea

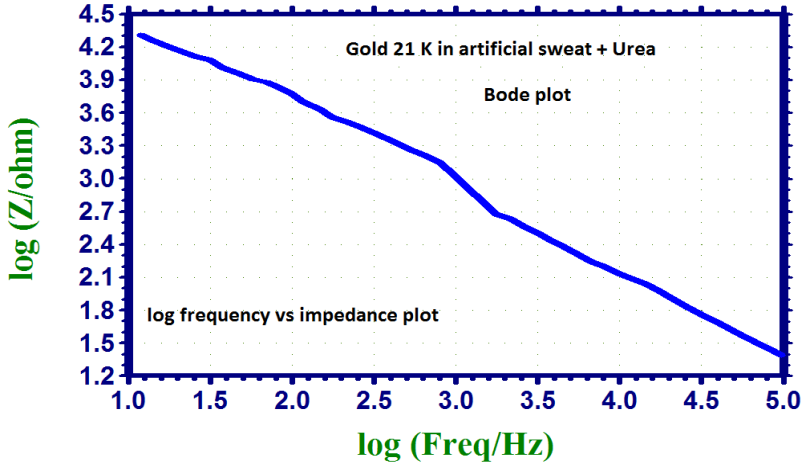

Figure 11. Log frequency vs. impedance plot of Gold 21K immersed in artificial sweat (AS) + Urea

Slika 11. Log frekvencije u odnosu na impedansu zlata 21K uronjenu u veštački znoj (AS) + urea

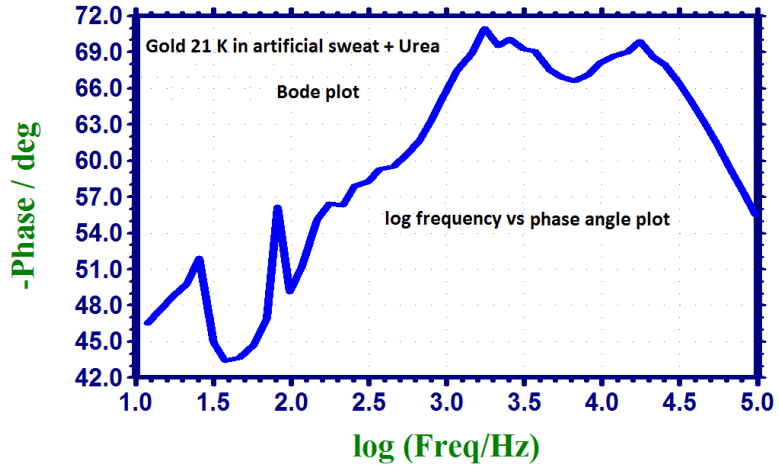

Figure 12. Log frequency vs. phase angle plot of Gold 21K immersed in artificial sweat (AS) + Urea

Slika 12. Log frekvencije u zavisnosti od faznog ugla zlata 21K uronjenog u veštački znoj (AS) + urea

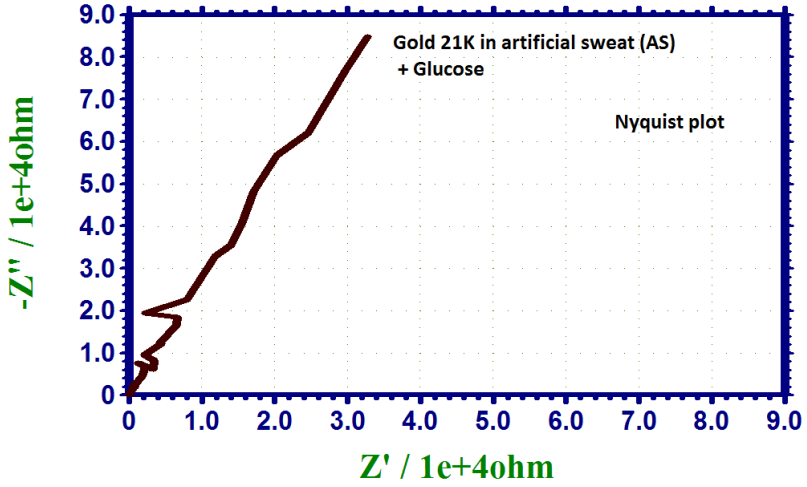

Figure 13. Nyquist plot of Gold 21K immersed in artificial sweat (AS) + Glucose

Slika 13. Nyquist-ov kriva zlata 21K uronjen u veštački znoj (AS) + glukoza

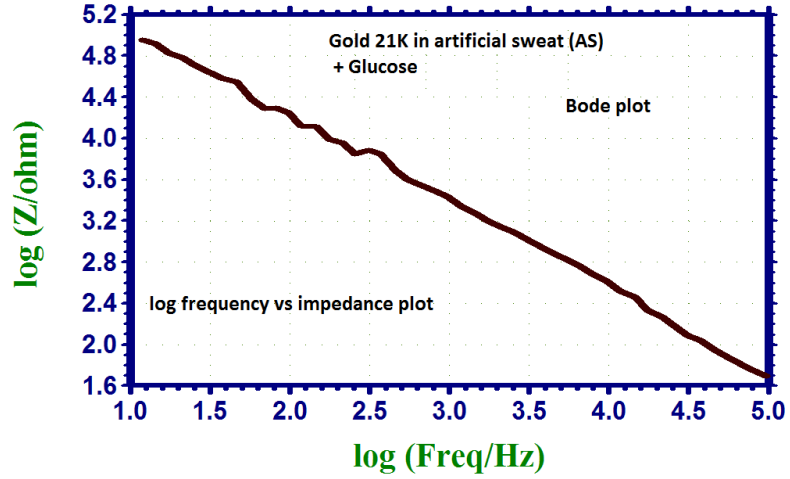

Figure 14. Log frequency vs. impedance plot of Gold 21K immersed in artificial sweat (AS) + Glucose

Slika 14. Log frekvencije u odnosu na impedansu zlata 21K uronjenog u veštački znoj (AS) + glukoza

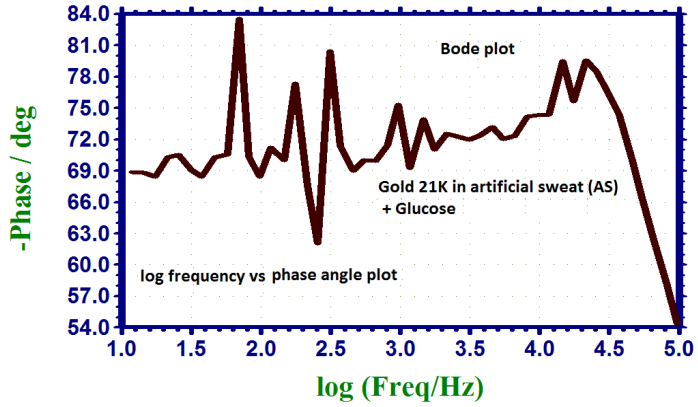

Figure 15. Log frequency vs. phase angle plot of Gold 21K immersed in artificial sweat (AS) + Glucose

Slika 15. Log frekvencije u odnosu na fazni ugao zlata 21K uronjenog u veštački znoj (AS) + glukoza

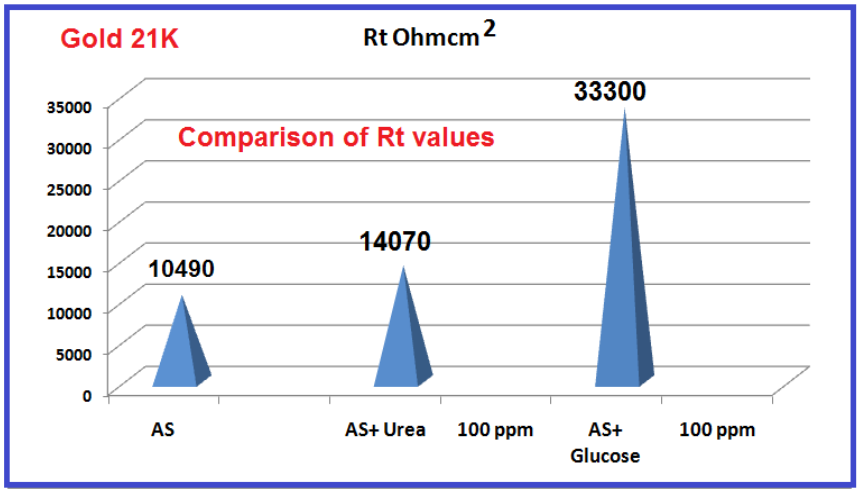

Figure 16. Comparison of R_t values of Gold 21K immersed in various test solutions

Slika 16. Poređenje vrednosti R_t zlata 21K uronjenog u različite testirane rastvore

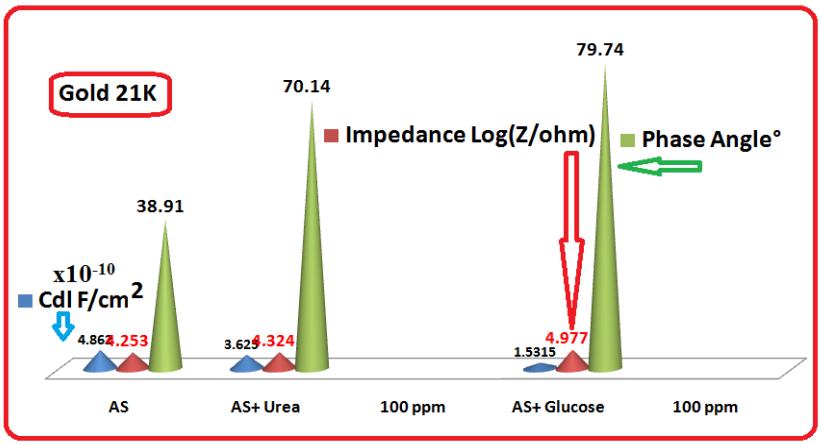

Figure 17. Comparison of corrosion parameters of Gold 21K immersed in various test solutions

Slika 17. Poređenje parametara korozije zlata 21K uronjenog u različita ispitivana rešenja

When corrosion resistance increases, R_t value increases, impedance value decreases whereas Cdl values increases, Impedance values decrease and phase angle values decrease (Scheme B).

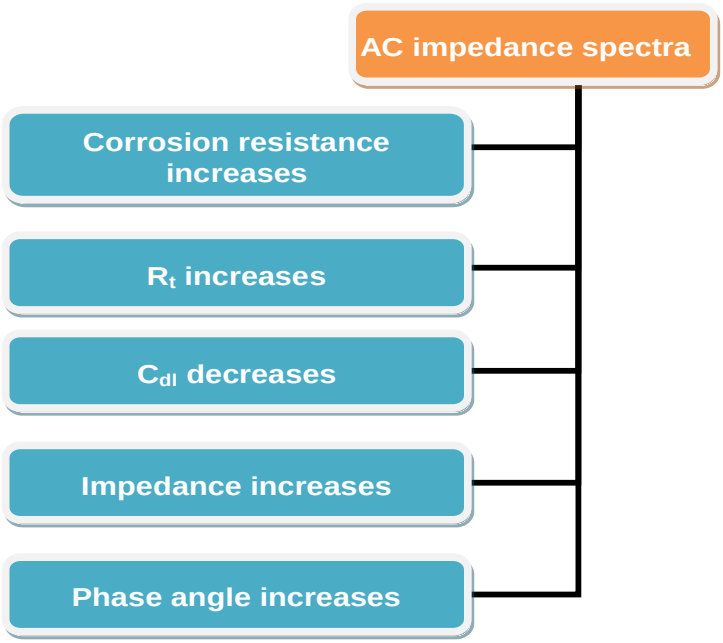

Scheme B. Correlation among corrosion parameters in AC impedance spectra

Šema B. Korelacija između parametara korozije u spektrima AC impedance

It is observed from Table 2, that in the presence of urea and glucose the corrosion resistance of Gold 21K in artificial sweat increases. This is revealed by the fact that in presence of urea/glucose, R_t value increases, impedance value increases, phase angle value increases and C_{dl} value decreases.

Implication

Corrosion resistance of Gold 21K alloy in artificial sweat increases in the presence of 100 ppm of *urea* and also100 ppm of glucose. Hence people having excess of *urea/glucose* in sweat need not worry about wearing ornaments made of Gold 21K alloy, such as wrist watches, rings , bangles etc.,.

4. SUMMARY AND CONCLUSIONS

Outcome of the study

Corrosion resistance of Gold 21K alloy in artificial sweat (AS), in the absence and presence of glucose and also urea has been investigated by polarization study and AC impendency spectra. It is inferred that corrosion resistance of Gold 21K alloy in artificial sweat increases in the presence of glucose and also urea. This is revealed by increase in LPR value, increase in R_t value, increase in impedance value, decrease in corrosion current, increase in phase angle and decrease in double layer capacitance value. Hence people having excess of urea/glucose in sweat need not worry about wearing ornaments made of Gold 21K alloy, such as wrist watches, rings, bangles etc., (Table 3).

Table 3. Summary of the study

Tabela 3. Rezime studije

Corrosion parameters	Artificial Sweat (AS)	AS + urea (100 ppm) (increases/decreases)	AS + D-Glucose (100 ppm) (increases/decreases)
LPR	103389	123437 (increases)	4817257(increases)
R_t	10490	14070(increases)	33300(increases)
Impedance	4.253	4.324(increases)	4.977(increases)
Corrosion current	4.036×10^{-7}	3.308×10^{-7} (decreases)	0.161×10^{-7}(decreases)
Double layer capacitance	4.862×10^{-10}	3.625×10^{-10}(decreases)	1.5315×10^{-10}(decreases)

Phase angle	38.91	70.14(increases)	79.74(increases)

5. REFERENCES

[1]H.Wang, J.Zheng, X.Sun, Y.Luo (2022) Tribo-corrosion mechanisms and electromechanical behaviours for metal implants materials of CoCrMo, Ti6Al4V and Ti15Mo alloys, Biosurface and Biotribology, 8(1),44-51.

[2]Y.Si, H.Liu, H.Yu, X.Jiang, D.Sun (2022) A heterogeneous $TiO_2/SrTiO_3$ coating on titanium alloy with excellent photocatalytic antibacterial, osteogenesis and tribocorrosion properties, Surface and Coatings Technology, 431,128008.

[3]P. Kochmański, M.Długozima, J.Baranowska (2022) Structure and Properties of Gas-Nitrided, Precipitation-Hardened Martensitic Stainless Steel, Materials, 15(3), 907.

[4]P.Lu, M.Wu, X.Liu, X.Miao, W.Duan (2022) A tribocorrosion investigation of SLM fabricated Ti6Al4V nanocomposites by laser rescanning and GO mixing, Rapid Prototyping Journal, 28(1), 32-40.

[5]X.-Y.Yu, X.-F.Sheng, T. Zhou, Z.Li, Y.Fu(2021) Corrosion behaviour of Cu-Zn-Ni-Sn imitation-gold copper alloy in artificial seawater and perspiration, Zhongguo Youse Jinshu Xuebao/Chinese Journal of Nonferrous Metals, 31(5), 1143-1155.

[6]S.J.Mary, D.Delinta, A.Ajila, S.K.Muthukumaran, S.Rajendran (2021) electrochemical behavior of various implantation biomaterials in the presence of various simulated body fluids–an overview, Zastita materijala, 62(3), 213-219.

[7]A.M.Elzohry, L.A.Khorshed, A.Attia, M.A.Adly, L.Z. Mohamed (2021) Chemical, Electrochemical and Corrosive Wear Behavior of Nickel-plated Steel and Brass-plated Steel Based Coins from Egypt in Artificial Sweat, International Journal of Electrochemical Science, 16, 1-16.

[8]S.A.Naser, A.A.Hameed, M.A.Hussein (2020) Corrosion behavior of some jewelries in artificial sweat, AIP Conference Proceedings, 2213, 020030.

[9]S.Huang, X.Song, C.Pan, G.Cao, Z.Wang (2020) Atmospheric corrosion behaviour of benzotriazole treated cu-based coins in synthetic sweat, International Journal of Electrochemical Science, 15, 7693-7708.

[10]X.Wang, G.Herting, Z.Wei, I.Wallinder, Y.Hedberg (2019) Bioaccessibility of nickel and cobalt in powders and massive forms of stainless steel, nickel- or cobalt-based alloys, and nickel and cobalt metals in artificial sweat, Regulatory Toxicology and Pharmacology, 106,15-26.

[11]S.C.Joycee, A.S.Raja, A.S.Amalraj, S.Rajendran (2021) Inhibition of corrosion of mild steel pipeline carrying simulated oil well water by Allium sativum (Garlic) extract, International Journal of Corrosion and Scale Inhibition, 10(3), 943-960.

[12]R.Dorothy, T.Sasilatha, S.Rajendran (2021) Corrosion resistance of mild steel (Hull plate) in sea water in the presence of a coating of an oil extract of plant materials,International Journal of Corrosion and Scale Inhibition, 10(2), 676-699.

[13]P.Shanthy, J.A.Thangakani, S.Karthika, S. Rajendran, J.Jeyasundari (2021) Corrosion inhibition by an aqueous extract of ervatamia divaricata, International Journal of Corrosion and Scale Inhibition, 10(1), 331-348.

[14]S.J.H.M.Jessima, A.Berisha, S.S.Srikandan, S. Subhashini (2020) Preparation, characterization, and evaluation of corrosion inhibition efficiency of sodium lauryl sulfate modified chitosan for mild steel in the acid pickling process, Journal of Molecular Liquids, 320, 114382.

[15]M.E.Belghiti, Y.E.Ouadi, S.Echihi, F.Bentiss, A. Dafali (2020) Anticorrosive properties of two 3, 5-disubstituted-4-amino-1, 2, 4-triazole derivatives on copper in hydrochloric acid environment: Ac impedance, thermodynamic and computational investigations, Surfaces and Interfaces, 21, 100692.

[16]A.S.Prabha, K.Kavitha, H.B.Shrine, S.Rajendran (2020) Inhibition of corrosion of mild steel in simulated oil well water by an aqueous extract of Andrographis paniculata, Indian Journal of Chemical Technology, 27(6), 452-460.

[17]J.J.M.Praveena, J.A.Clara, S.Rajendran, A.J. Amalraj, (2021) Inhibition of corrosion of mild steel in well water by an aqueous extract of soapnut (Sapindus Trifoliatus) , Materials Protection, 62(4), 277-290.

[18]V.D.Jeslina, S.J.Kirubavathy, A.Al-Hashem, R.M.Joany, C.Lacnjevac (2021) Inhibition of corrosion of mild steel by an alcoholic extract of a seaweed Sargassum muticum, Zastita materijala, 62(4), 304-315.

[19]S.Y. Al-Nami, A.S.Fouda (2020) Corrosion inhibition effect and adsorption activities of methanolic myrrh extract for cu in 2 M HNO_3,International Journal of Electrochemical Science, 15(2),1187-1205.

[20]A.Ch.Catherine Mary, J.Jeyasundari, V.R.N. Banu, S.Senthil Kumaran, A.P.Pascal Regis (2020) Corrosion behavior of orthodontic wires in artificial saliva with presence of beverage (Book Chapter),

Nanotechnology in the Beverage Industry: Fundamentals and Applications, p.471-504

IZVOD

UTICAJ UREE I GLUKOZE NA OTPORNOST LEGURE ZLATA 21K NA KOROZIJU U PRISUSTVU VEŠTAČKOG ZNOJA

Otpornost na koroziju legure zlata 21K uronjene u veštački znoj u odsustvu i prisustvu 100 ppm uree i 100ppm D-glukoze je ispitana proučavanjem polarizacije i spektara impedanse naizmenične struje. Primećeno je da se povećava otpornost na koroziju legure zlata 21K uronjene u veštački znoj u prisustvu 100 ppm uree/D-glukoze. Otuda se zaključuje da ljudi koji nose ukrase od legure zlata 21K ne moraju da brinu o višku uree/D-glukoze u svom znoju. Kada se legura zlata 21K potopi u veštački znoj u prisustvu 100 ppm uree, vrednost otpora linearne polarizacije se povećava sa 103389 Ohmcm^2 na 123437Ohmcm^2; struja korozije opada sa 4,036 k10^{-7}A/cm^2 na 3,308 k10^{-7}A/cm^2; vrednost otpora prenosa naelektrisanja se povećava sa 10490 Ohmcm^2 na 14070 Ohmcm^2; vrednost impedanse se povećava sa 4,253 na 4,324; kapacitivnost dvostrukog sloja se smanjuje sa 4,862k10^{-10} F/cm^2 na 3,625k10^{-10}F/cm^2, a fazni ugao se povećava sa 38,91° na 70,14°. Kada se legura zlata 21K potopi u veštački znoj u prisustvu 100ppm D-glukoze, vrednost otpora linearne polarizacije se povećava sa 103389 Ohmcm^2 na 4817257Ohmcm^2; struja korozije se smanjuje sa 4,036 k10^{-7}A/cm^2 na 0,161k10^{-7}A/cm^2; otpor prenosa naelektrisanja se povećava sa 10490 Ohmcm^2 na 33300 Ohmcm2; vrednost impedanse se povećava sa 4,253 na 4,977; kapacitivnost dvoslojnog sloja se smanjuje sa 4,862k10^{-10} F/cm^2 na 1,5315k10^{-10} F/cm^2, a fazni ugao se povećava sa 38,91° na 79,74.

Ključne reči: *otpornost na koroziju, termoaktivna legura, legura zlata 21K, veštački znoj, studija polarizacije, spektri impedanse naizmenične struje.*

Naučni rad

Rad primljen: 30. 03. 2022.

Rad prihvacen: 14. 04. 2022.

Rad je dostupan na sajtu: www.idk.org.rs/casopis